Inelastic Scattering with Chebyshev Polynomials and Preconditioned Conjugate Gradient Minimization

Burcin Temel, Greg Mills, and Horia Metiu*

Department of Chemistry and Biochemistry, University of California, Santa Barbara, California 93106

Received: July 30, 2007; In Final Form: January 5, 2008

We describe and test an implementation, using a basis set of Chebyshev polynomials, of a variational method for solving scattering problems in quantum mechanics. This minimum error method (MEM) determines the wave function Ψ by minimizing the least-squares error in the function $(\hat{H}\Psi - E\Psi)$, where E is the desired scattering energy. We compare the MEM to an alternative, the Kohn variational principle (KVP), by solving the Secrest−Johnson model of two-dimensional inelastic scattering, which has been studied previously using the KVP and for which other numerical solutions are available. We use a conjugate gradient (CG) method to minimize the error, and by preconditioning the CG search, we are able to greatly reduce the number of iterations necessary; the method is thus faster and more stable than a matrix inversion, as is required in the KVP. Also, we avoid errors due to scattering off of the boundaries, which presents substantial problems for other methods, by matching the wave function in the interaction region to the correct asymptotic states at the specified energy; the use of Chebyshev polynomials allows this boundary condition to be implemented accurately. The use of Chebyshev polynomials allows for a rapid and accurate evaluation of the kinetic energy. This basis set is as efficient as plane waves but does not impose an artificial periodicity on the system. There are problems in surface science and molecular electronics which cannot be solved if periodicity is imposed, and the Chebyshev basis set is a good alternative in such situations.

1. Introduction

Scattering problems in quantum mechanics have been approached by a range of computational methods, which may be divided into two main categories, time-independent (TI) and time-dependent (TD), depending on which version of the Schrödinger equation is solved. In a TI method, one specifies the scattering energy, and then finds the wave function that corresponds to it. From this, the state-to-state resolved differential cross sections may be extracted; this information is implied by the **S** matrix at the given energy E. This allows a direct comparison to experiments, which obtain these scattering amplitudes at a known energy. Also, experiments measuring photon emission or absorption by colliding molecules require for their interpretation a detailed knowledge of the wave function at a particular energy. In a TD method, the output contains a superposition of many energies, and one thus obtains a scattering spectrum in an energy window. This method also allows for comparison with experiments obtaining, for example, spectroscopic information.

Computational methods for scattering have been reviewed recently by Althorpe and Clary.[1] This review contains a clear summary of various approaches, together with many tests against gas-phase experiments.

In the present paper, we describe a new TI method, using Chebyshev polynomials as a basis set, which allows one to avoid some of the common limitations of TI methods while retaining the advantage of using a TI method to obtain state-to-state scattering amplitudes, which are less conveniently available and often less accurate when obtained by a TD method. This use of Chebyshev functions as a spatial basis set is not to be confused with their use to describe the time dependence of the wave function.[1,2] In order to show the Chebyshev basis set in context, we discuss several computational aspects of the scattering calculation (but for more general details, see ref 1). We illustrate the present method by solving an example two-dimensional problem, the Secrest−Johnson model for H_2 + He vibrationally inelastic scattering.[3,4]

The most important numerical features of any computation are the scaling of computer time with problem size and the accuracy of the final answer. The Chebyshev basis set[5−8] has implications for both.

Concerning scaling, a TD method involves a matrix−vector multiplication for some number of time steps. This method scales as $O(N^2)$ per step, where N is the number of basis functions (or grid points), with a prefactor that includes the number of time steps needed. The matrix is based on the Hamiltonian operator and is usually sparse; therefore, the above scaling is an upper bound to the actual scaling obtained. A TI method involves either a direct matrix inversion, which scales as $O(N^3)$, or a residual minimization method (RMM), which scales as $O(N^2)$ (or less) per iterative step but might require many steps to converge. If results at several energies are desired, the prefactor includes the energy resolution.

With a Chebyshev basis set, applying the Hamiltonian to the wave function scales as only $O(N \log N)$ instead of $O(N^2)$ because an analogy with cosine functions allows us to use the fast Fourier transform in its cosine form (the FCT).[9] Also, the very large Hamiltonian matrix need not be stored in memory. This means that the Chebyshev method can be extended efficiently to systems with several degrees of freedom. However, the grid must still be "rectangular" because we have an outer product of functions of one variable (see section 3), whereas

* To whom correspondence should be addressed.

10.1021/jp0760307 CCC: $40.75
Published on Web 02/28/2008

in, for example, discrete variable representation (DVR) methods, a "pruned" grid may be used, with grid points placed only where the potential energy is not too high.[10] The need for a rectangular grid is a disadvantage in high-dimensional cases since the number of grid points becomes large; for a 6D problem and with $N = 32$ grid points in each dimension, the wave function would have $\sim 10^9$ entries.

No strict minimum principle is known for scattering states.[11] Variational principles do exist, for example, several varieties of the Kohn variational principle (KVP),[12] particularly the **S** matrix KVP.[10,13−28] Using the KVP requires finding a stationary point (a saddle point) of a functional of the wave function, and this typically means a (slow) matrix inversion. There are also instabilities associated with this approach, for example, spurious resonances.[29−31]

Instead of the KVP, we use a RMM-type method,[32−42] in which the residual, $H\Psi - E\Psi$, is driven to zero by iterative minimization of the least-squares error

$$F[\Psi] = \langle H\Psi - E\Psi | H\Psi - E\Psi \rangle \quad (1)$$

For clarity, we call the present method a minimum error method (MEM).

We also use the **R** matrix description of scattering amplitudes rather than the **S** matrix; these and the scattering phase shifts contain the equivalent information,[43] but the **R** matrix uses real numbers, and the **S** matrix uses complex numbers, giving some computational advantage to the former. Also, the **R** matrix is symmetric and thus allows for a test of the method because, for example, the (1,2) and (2,1) elements are obtained in different calculations and should come out the same if the method is accurate. The **R** matrix appears to be unstable within the KVP but is amenable to treatment by a RMM.

The iterative method is only better than a direct matrix inversion if the number of steps required to converge is not too large (and is not proportional to the number of grid points). The matrix in the RMM contains the Hamiltonian squared (see eq 1) and thus the d/dx operator to the fourth power, which makes it ill-conditioned (i.e., its eigenvalues span a wide range). Attempting to iteratively solve an ill-conditioned problem will take a very large number of steps, and worse, the answer obtained will be inaccurate. This happens because the steps taken eventually involve extremely small changes in the trial wave function, and at some point, these changes fall below the level of the computer's round-off error. At this point, the trial wave function stops changing, and even though a very accurate wave function does exist, this solution cannot be reached.

Avoiding this problem requires preconditioning (PC), which reduces the apparent condition number of the matrix by applying a fast, approximate inversion of the matrix.[6,7,44,45] PC has been used in scattering calculations.[40,46] For the Chebyshev basis set, we have developed a good preconditioner,[47] which we use in the present work. The accuracy obtained is determined by (1) the boundary conditions (BC) and (2) the quality and compatibility of the differentiation and integration methods.

For scattering calculations, the BC are especially problematic because the wave function at an outer boundary should not approach zero; instead, it should become a linear combination of asymptotic scattering states. If no BC are supplied, the wave function will scatter off of the boundaries of the grid, giving fictitious results. Thus, for TD[10,48] and some TI[49] methods, a "complex absorbing potential" (CAP)[50,51] is used at the boundaries. The CAP requires extra grid points, across which the wave function is damped smoothly to zero while altering it only slightly inside of the main interaction region. Still, there is usually weak scattering off of the boundaries, and components of the wave function at different energies respond to the CAP differently,[52,53] making the final answer often dependent on the particular CAP used. If the basis set is accurate enough to give an error in the wave function of, for example, 10^{-4}, then any scattering off of the boundary above this amount will dominate the total error of the calculation.

A TI method contains only one energy, which makes accurate scattering results easier to achieve, especially in the case of resonances (long-lived scattering states that have enough energy to escape),[54] for which it may be problematic within a TD method to propagate the wave function long enough to resolve the resonance (see ref 1). The asymptotic scattering states are known (see below), and we can make the Chebyshev representation of the wave function match exactly the asymptotic states at the outer boundary of the grid. This match is achieved by a vector projection, which requires negligible CPU time and no extra grid points. This is possible because the Chebyshev basis set describes a smooth function, which may take arbitrary values at the boundaries, and gives accurate derivatives up to and including the boundary points; this is a consequence of the nonuniform Gauss−Lobato grid, which is dense near the boundaries.[6−8] As a result, fictitious scattering off of the BC does not occur in the present method.

In the past,[14,15,17−19] a power series (the set of polynomials $\{1, x, x^2, ...\}$) has been used as a basis set. These functions do not oscillate and thus have trouble describing oscillations. Although they are isomorphic to the Chebyshev basis set (both are polynomials), the coefficients typically become very large and lead to inaccuracy, and the positions of the grid points also matters. In our earlier work,[47] we found that the power series basis set, with a uniform grid, does not converge; see Boyd for discussion.[7]

On the other hand, Chebyshev polynomials oscillate "uniformly" throughout the x interval $[-1,1]$, which makes the expansion of a function numerically stable. They form a complete and orthogonal basis set and thus give results that converge to a definite limit as the number of basis functions increases. A Fourier-type transform exists for the Chebyshev polynomials, which allows fast derivative calculations with the accuracy of a Fourier series but without the implied periodicity of the Fourier functions.[6,7] They are thus more accurate than a finite difference (FD) definition of the derivative, for the same number of grid points. Integration (quadrature) is done naturally by integrating the basis functions; thus, differentiation and integration are compatible with each other.

Also commonly used in scattering calculations are various DVR methods,[10,41,46,55,56] which we do not summarize here. Those that use a uniform grid may expect to have trouble with the derivative near the boundaries, in common with uniform-grid FD methods,[7,57] and Fourier methods applied to discontinuous functions.[58] Some nonuniform grid calculations for scattering have been described,[59,60] which may allow for more accurate handling of the boundary conditions.

2. The Model

As a test problem, we use the Secrest−Johnson model of a collinear three-atom collision (a scatterer hitting a diatomic molecule), as illustrated in Figure 1.

The Hamiltonian in the Secrest−Johnson form is

$$\hat{H} = -\frac{1}{2m}\left(\frac{\partial^2}{\partial \tilde{x}^2}\right) - \frac{1}{2}\left(\frac{\partial^2}{\partial \tilde{y}^2}\right) + \frac{1}{2}(\tilde{y} - \tilde{y}_{eq})^2 + V_0 \exp[-\gamma(\tilde{x} - \tilde{y})] \quad (2)$$

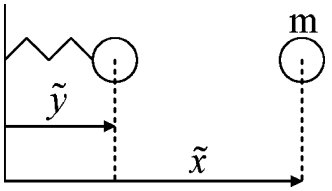

Figure 1. Reduced coordinates of the Secrest−Johnson model.

Here, $\hat{H}$ and $\tilde{x}$ and $\tilde{y}$ are in atomic units, and m is a mass ratio, which applies to the $\tilde{x}$ (i.e., scattering) coordinate and is defined by

$$m = \frac{m_A m_C}{m_B(m_A + m_B + m_C)} \tag{3}$$

Here, m_A is the mass of the scatterer, and m_B and m_C are the masses of the molecule. For H_2 + He scattering, $m = 2/3$ and $\gamma = 0.3$ in eq 2. V_0 determines the distance of the classical turning point of the collision from the oscillator in the interaction potential. This only shifts the $\tilde{x}$ coordinate and has no physical consequences; we use $V_0 = 12.0$ for convenience. The energy E of the scattering state is also measured in atomic units

$$E = \frac{k_n^{\,2}}{2m} + \epsilon_n \tag{4}$$

$$\epsilon_n = n + 1/2 \qquad n = 0, 1, 2, ..., N_{vib} \tag{5}$$

where k_n is the wave vector that describes the kinetic energy of scattering from the nth vibrational level of the diatomic molecule having energy ϵ_n according to eq 5.

E is fixed throughout the scattering event, and thus, a higher translational kinetic energy of the scatterer is associated with a lower vibrational state of the molecule and vice versa. N_{vib} is the highest vibrational state of energy less than E, which therefore may be excited during the scattering event. The k_n is found from eqs 4 and 5 after E and n are specified; a scattering channel (indexed by n) is called open if the resulting k_n is real, that is, $n \le N_{vib}$, and channels with imaginary k_n are closed. We perform calculations for two cases, $E = 3$ and 6, with three and six open channels, respectively.

The "physical" coordinates $\tilde{x}$ and $\tilde{y}$ have ranges $[0, \tilde{x}_{max}]$ and $[0,\tilde{y}_{max}]$. In this paper, these are $\tilde{x}_{max} = 20$ and $\tilde{y}_{max} = 16$, with $\tilde{y}_{eq} = 8$. However, in the Chebyshev representation, we need new coordinates (x,y) in the range of $[-1,1]$. We scale every function into this range as described in our previous work.[47] Rewriting the Hamiltonian in the Chebyshev coordinates

$$\hat{H} = -\frac{1}{2m}\left(\frac{2}{\tilde{x}_{max}}\right)^2\left(\frac{\partial^2}{\partial x^2}\right) - \frac{1}{2}\left(\frac{2}{\tilde{y}_{max}}\right)^2\left(\frac{\partial^2}{\partial y^2}\right) + \frac{1}{2}\left(\frac{\tilde{y}_{max}}{2}\right)^2 y^2 + V_0 \exp\left[-\gamma\left(\frac{\tilde{x}_{max}}{2}x - \frac{\tilde{y}_{max}}{2}y - \tilde{y}_{eq}\right)\right] \tag{6}$$

3. The Representation of the Wave Function

The wave function $\Psi(x_i,y_j)$ (two-dimensional throughout) is defined at grid points $\{x_i,y_j\}$ with $i = 0, ..., N$ and $j = 0, ..., M$, and the values on the boundary are fixed (to zero). The variables in the problem are thus $\Psi(x_i,y_j)$ for $i = 1, ..., N - 1$ and $j = 1, ..., M - 1$ and the elements in one column of the **R** matrix, which describe the phase of the asymptotic part of the wave function. These are varied to minimize the error, F, in eq 1.

The trial wave function is

$$\Psi_t(x,y) = f(x)\,\Psi_I(x,y) + g(x)\,\Psi_a(x,y) \tag{7}$$

where $f(x)$ and $g(x)$ are cutoff functions, $\Psi_I(x,y)$ is the wave function in the region where the projectile and the target interact, and $\Psi_a(x,y)$ is the wave function in the asymptotic region (no interaction).

If the system is initially in the ground vibrational state, $n = 0$, and the incoming wave vector k_i is such that only three channels are open (i.e., the vibrational quantum number after the collision could be $n = 0, 1, 2$), then the asymptotic wave function Ψ_a is

$$\Psi_a(x,y) = k_i^{-1/2}[\sin(k_i x) + R_{00}\cos(k_i x)]\varphi_0(y) + k_1^{-1/2}R_{01}\cos(k_1 x)\,\varphi_1(y) + k_2^{-1/2}R_{02}\cos(k_2 x)\,\varphi_2(y) \tag{8}$$

and k_1 and k_2 are the wave vectors, after the collision, if the oscillator is excited to the vibrational state $n = 1$ or 2, respectively. R_{00}, R_{01}, and R_{02} are the unknown elements of the **R** matrix for the incoming wave vector k_i and the initial oscillator state $n = 0$. The $\varphi_n(y)$ is a harmonic oscillator eigenstate

$$\varphi_n(y) = (\pi^{1/2}2^{n-1}n!)^{-1/2}H_n(y)\exp[-y^2/2] \qquad n = 0, 1, ... \tag{9}$$

where $H_n(y)$ is a Hermite polynomial.

Computations with the **R** matrix asymptotic wave functions are easier than those using the **S** matrix because real number arithmetic is used. The **R** matrix obtained from the functional minimization is used to calculate the **S** matrix and transition probabilities; these quantities are connected to each other by exact relationships.[43] The **R** matrix is real and symmetric.

If the oscillator is initially in an excited state (e.g., $n = 1$), then the asymptotic wave function is The variational calculation

$$\Psi_a(x,y) = k_0^{-1/2}R_{10}\cos(k_0 x)\,\varphi_0(y) + k_i^{-1/2}[\sin(k_i x) + R_{11}\cos(k_i x)]\varphi_1(y) + k_2^{-1/2}R_{12}\cos(k_2 x)\,\varphi_2(y) \tag{10}$$

of (R_{00}, R_{01}, R_{02}) is independent from that of (R_{10}, R_{11}, R_{12}). However, since the **R** matrix is symmetric, R_{ij} and R_{ji} obtained in independent calculations must be equal. Checking this equality is a test of the stability of the numerical method.

It is important to choose the correct cutoff functions in eq 7. First, $g(x)$ conveys a fraction of the asymptotic wave functions into the interaction region and can be any function that goes to zero at small x (the closed boundary). This is because whatever $g(x)$ is, the correct $\Psi_\tau(x,y)$ can always be obtained by choosing $\Psi_I(x,y)$ correctly, and by driving the error to zero, we achieve this. Intuitively, $f(x)$ should approach zero at the open boundary, but surprisingly, this makes the convergence worse. If a cutoff function $f(x)$ is used, then some of the variables $\Psi_I(x_i,y_j)$ near the open boundary get multiplied by a small number, for example, 10^{-6}, and this unbalanced situation slows down the convergence and also reduces the final accuracy. In fact, we do not need a cutoff function for $\Psi_I(x,y)$ because the BC at the open boundary are set exactly by matching $\Psi_t(x,y)$ to $\Psi_a(x,y)$ there by a method described below. This matching is accurate and efficient for Chebyshev polynomials and leaves no work for the cutoff function to do.

Therefore, we use

$$f(x) = 1$$

$$g(x) = \frac{1}{2}(1 + \tanh[\beta(x - \gamma)]) \qquad \beta = 0.5,\ \gamma = 15 \quad (11)$$

We found, as expected, that the choices

$$f(x) = \exp(-\alpha x) \qquad \alpha = 0.5 \text{ with } g(x) = 1 - f(x) \quad (12)$$

$$f(x) = 1 - \frac{1}{2}\{1 + \tanh[\beta(x - \gamma)]\}$$
$$\beta = 0.5,\ \gamma = 15 \text{ with } g(x) = 1 - f(x) \quad (13)$$

$$f(x) = 1 \text{ with } g(x) = 1 - \exp(-\alpha x) \qquad \alpha = 0.5 \quad (14)$$

were less efficient.

At the inner boundary, the total wave function (hence also $\Psi_I(x,y)$) obeys the scaling law

$$\Psi_t(x,y) \xrightarrow[x\to 0]{} x^{l+1} \quad (15)$$

where $l = 0$ for s-wave scattering. At some point, x_{max}, beyond which the interaction is zero, we must have

$$\Psi_t(x,y) \xrightarrow[x\to x_{max}]{} \Psi_a(x,y) \quad (16)$$

which means that for all values of y

$$\Psi_I(x_{max},y) = 0 \quad (17)$$

We impose eqs 15 and 17 and the corresponding requirements at the y_{min} and y_{max} by setting $\Psi_I(x,y) = 0$ at each boundary point. In addition, we must impose the condition

$$\left.\frac{d\Psi_I}{dx}\right|_{x=x_{max}} = 0 \quad (18)$$

which is equivalent to

$$\left.\frac{d\Psi_t}{dx}\right|_{x=x_{max}} = \left.\frac{d\Psi_a}{dx}\right|_{x=x_{max}} \quad (19)$$

This ensures that the flux is entirely accounted for by the asymptotic form of the wave function. Failure to achieve this would result in an incorrect **R** matrix. The boundary condition eq 18 is implemented by a method that we developed (see Appendix B).

We represent the wave function in the interaction region, $\Psi_I(x,y)$, by a sum of products of Chebyshev polynomials. The Chebyshev representation of a function is written in the literature in a variety of forms. The form used here is shown below. A function $f(x)$, with $x \in [-1,1]$ is expanded in coefficients $\{b_n\}$

$$f(x_i) = \frac{b_0}{2}T_0(x_i) + \sum_{n=1}^{N-1} b_n T_n(x_i) + \frac{b_N}{2}T_N(x_i) \equiv \sum_{n=0}^{N} \eta_n b_n T_n(x_i) \quad (20)$$

with

$$\eta_n = \begin{Bmatrix} 1/2 & \text{if } n = 0 \text{ or } N \\ 1 & \text{otherwise} \end{Bmatrix} \quad (21)$$

$T_n(x)$ is a Chebyshev polynomial of the first kind, which may be written as

$$T_n(x) = \cos(n \arccos(x)) \quad (22)$$

We use a Gauss−Lobato grid[7,8]

$$x_i = \cos(i\pi/N) \quad i = 0, 1, ..., N \quad (23)$$

and the coefficients $\{b_n\}$ are calculated from $f(x)$ by

$$b_n = \frac{2}{N}\sum_{i=0}^{N} \eta_i T_n(x_i) f(x_i) \quad (24)$$

Using eqs 20 and 24 allows one to move back and forth between the two representations of $f(x)$, either sampled at $N + 1$ grid points or expanded as $N + 1$ Chebyshev coefficients. In practice, this is done not with eqs 20 and 24, which would require $O(N^2)$ operations, but with a fast Chebyshev transform (FCT), which requires $O(N \log N)$ operations. The FCT is operationally identical to the fast cosine transform.[9] The generalization to two dimensions is straightforward.

4. The Conjugate Gradient Minimization

To find the correct wave function, we minimize the functional F in eq 1. In the asymptotic region, we satisfy $\hat{H}\Psi = E\Psi$ by making the correct choice of Ψ_a, which leaves F to be integrated throughout the interaction region. Scaling the variables to bring them into the range of $[-1,1]$ brings a constant in front of the integral, which we drop because all we need from F is the wave function which minimizes it. We then have

$$F = \int_{-1}^{1}\int_{-1}^{1} dx\, dy\, [(\hat{H} - E)\Psi_t(x,y)]^2 \quad (25)$$

Now, the integrand $g(x,y) = [(\hat{H} - E)\Psi_t(x,y)]^2$ is a function of x and y, and we expand both dimensions in Chebyshev polynomials

$$\begin{aligned} F &= \int_{-1}^{1}\int_{-1}^{1} dx\, dy\, g(x,y) \\ &= \sum_{\alpha=0}^{N}\sum_{\beta=0}^{M} c_{\alpha\beta}\int_{-1}^{1}\int_{-1}^{1} dx\, dy\, T_\alpha(x)\, T_\beta(y)\eta_\alpha\eta_\beta \\ &= \sum_{\alpha=0}^{N}\sum_{\beta=0}^{M} c_{\alpha\beta}\frac{2}{1-\alpha^2}\frac{2}{1-\beta^2}\eta_\alpha\eta_\beta \qquad \alpha, \beta \text{ even} \end{aligned} \quad (26)$$

where we have used eq 20 twice, and the last equality follows from

$$\begin{aligned} \int_{-1}^{1} dx\, T_\alpha(x) &= \frac{2}{1-\alpha^2} \qquad \alpha \text{ even} \\ &= 0 \qquad \alpha \text{ odd} \end{aligned} \quad (27)$$

Using eq 24 for each dimension, we can rewrite $c_{\alpha\beta}$ in eq 26 in terms of $g(x_i,y_j)$. The result, after rearrangement, is

$$F = \sum_{i=0}^{N}\sum_{j=0}^{M} [(\hat{H} - E)\Psi_t]_{i,j} w_i w_j [(\hat{H} - E)\Psi_t]_{i,j} \quad (28)$$

where the subscript i,j means that the quantity in the square bracket must be evaluated at the grid point (x_i,y_j) determined by eq 23. The integration weights in the x coordinate are

$$w_i = \frac{2}{N}\sum_{\alpha=0}^{N} \eta_i\eta_\alpha \frac{2}{1-\alpha^2} T_\alpha(x_i) \quad (29)$$

To calculate $\{w_j\}$ for the y coordinate, replace N with M and x_i with y_j in eq 29. These weights need to be calculated only once.

The desired wave function is obtained by minimizing F in eq 28 with respect to each of its variables, which we collect into a single "vector" z

$$z = \{\Psi_I(1,1), ..., \Psi_I(N-1, M-1), R_{00}, ..., R_{0m}\} \quad (30)$$

We explain here the procedure for an example where the oscillator is in the lowest energy state, for which the **R** matrix elements are (R_{00}, R_{01}, ..., R_{0m}), where m is the number of open channels. The use of the wave function at the grid points as unknown quantities allows an easy implementation of the boundary conditions; the values of the wave functions at the border are kept equal to those required by the boundary conditions. If we used the coefficients of the Chebyshev expansion as the variables, the boundary conditions would require the additional work of solving a system of $(2N + 2M)$ linear equations at every iteration step in the minimization algorithm.

To find the value of z that minimizes $F(z)$, we use the conjugate gradient (CG) procedure.[9] Since the literature contains many implementations, we describe briefly the one used here in Appendix A. Appendix B explains a new method for the efficient implementation of the requirement that the derivative of $\Psi_I(x,y)$ should be zero when $x = x_{max}$. The implementation of the CG method requires an efficient evaluation of $F(z)$. The only part here that is not straightforward is the accurate evaluation of the terms containing the kinetic energy in $[(\hat{H} - E)\Psi_I]_{i,j}$ when we know the values of $\Psi_I(x,y)$ at a set of grid points. We have developed an efficient procedure for performing this calculation, which is explained in Appendix C. The efficient evaluation of the gradient of $F(z)$ requires some care, and a new method for performing it is explained in Appendix D. Finally, the gradient is preconditioned using a method explained in our previous work.[47]

5. Results

5.A. The Transition Probabilities and the R Matrix. We have tested the method described above for the inelastic scattering problem of Secrest and Johnson[3,61] for the collinear $He-H_2$ system.

The minimization procedure gives the **R** matrix, and we calculate the **S** matrix by

$$\mathbf{S} = \frac{I + iR}{I - iR} \quad (31)$$

where I is the unit matrix and the denominator implies a matrix inverse. The transition probabilities, from initial state i to final state j, are

$$P_{ij} = |S_{ij}|^2 \quad (32)$$

We compare our results with those obtained by the KVP[23] and with the results of the numerical integration by Miller and Jansen op de Haar[14] and by Secrest and Johnson.[4] Unfortunately, there are no exact results for this model, and the accuracy of the numerical calculations is not known. The two numerical methods[14,23] to which we compare our results differ from each other. However, these differences do not exceed the accuracy expected in scattering experiments.

The calculated transition probabilities are shown in Tables 1 and 2. In Table 1, the MEM achieves the closest values to the exact calculation with $N = M = 32$, meaning there are $33^2 = 1089$ grid points. In Table 2, the KVP performs the best, while the MEM also attains reasonably good results. In these calculations, the KVP uses a shorter scattering range ($\tilde{x}_{max} = 10$ au) than ours ($\tilde{x}_{max} = 20$ au). Using a smaller range requires fewer basis functions and grid points, but it is important to consider where the interaction potential really becomes negligible. Hence, we took $\tilde{x}_{max} = 20$ au to make sure that there is no interaction in the asymptotic region.

TABLE 1: Transition Probabilities for the Secrest−Johnson Model with an Incident Energy of $E = 3.0$ au and Three Open Channels[a]

	MEM-Cheb (this work)	SKVP (ref 23)	numerical (ref 14)	exact (ref 3)
P_{12}	0.25×10^{-1}	0.30×10^{-1}	0.30×10^{-1}	0.22×10^{-1}
P_{23}	0.13×10^{-2}	0.15×10^{-2}	0.16×10^{-2}	0.09×10^{-2}
P_{13}	0.90×10^{-5}	0.87×10^{-5}	1.13×10^{-5}	NA

[a] The minimum error method with a Chebyshev representation and preconditioned conjugate gradient minimization (MEM-Cheb) uses $N = M = 32$ grid points; the **S** matrix KVP uses $N = 18$ basis functions.

TABLE 2: Same as Table 1, but $E = 6.0$ au[a]

	MEM-Cheb	SKVP (ref 23)	numerical (ref 14)	exact (ref 3)
P_{12}	0.38	0.39	0.39	0.39
P_{25}	0.41×10^{-3}	0.41×10^{-3}	0.39×10^{-3}	NA
P_{34}	0.22	0.23	0.23	0.23
P_{36}	0.32×10^{-5}	0.19×10^{-5}	0.20×10^{-5}	NA

[a] There are six open channels, and $N = M = 64$ grid points are used in MEM-Cheb. The **S** matrix KVP uses $N = 25$ basis functions.

TABLE 3: Elements of the R Matrix Shown for MEM-Cheb, with $E = 3.0$ au and $N = M = 32$ Grid Points, and F, the Minimum Error for Each Row Minimization[a]

	column 1	column 2	column 3	F	A	B
row 1	0.48	−0.10	-8.66×10^{-4}	3.54×10^{-5}	466	2873
row 2	−0.11	0.65	2.49×10^{-2}	4.61×10^{-4}	455	2615
row 3	-1.61×10^{-4}	1.94×10^{-2}	−0.25	7.34×10^{-3}	353	2153

[a] Columns A and B give the number of CG iterations required with and without preconditioning.

Each row of the **R** matrix is solved independently. With this approach, we can test whether the **R** matrix is symmetric. In Tables 3 and 4, we show the **R** matrices for the two energies. R_{ij} and R_{ji} approach each other as we increase the basis set size. $N = M = 32$ grid points are sufficient for the case of three open channels (see Table 3), but $N = M = 64$ grid points are needed in the case of six open channels (see Table 4). This is not surprising; the higher energy means the wave function varies more rapidly in the interaction region. Tables 3 and 4 also show the number of iteration steps that the conjugate gradient minimization takes with and without preconditioning.

5.B. The Convergence and Numerical Stability of Conjugate Gradient Minimization. Since the functional F is quadratic in the unknown quantities, taking derivatives and setting them to zero leads to a set of linear equations. The matrix in this system is very ill-conditioned; we have calculated its eigenvalues numerically and found them to differ by 7 orders of magnitude, indicating that a straightforward attempt to minimize F will converge very slowly. Therefore, some preconditioner is needed.

A preconditioner, in general, is designed to accelerate the convergence by improving the condition number of the matrix. There is no general method for preconditioning, and each specific problem must be treated separately.[6] We have used here an adaptation of the preconditioning that we applied earlier to a one-dimensional problem,[47] as explained in Appendix E.

TABLE 4: Same as Table 3, but $E = 6.0$ au and $N = M = 64$[a]

	column 1	column 2	column 3	column 4	column 5	column 6	F	A	B
row 1	1.13	-0.63	-4.50×10^{-3}	-2.58×10^{-2}	-9.97×10^{-4}	3.60×10^{-2}	6×10^{-12}	2186	10^4
row 2	-0.63	-7.76×10^{-3}	-0.52	-7.08×10^{-2}	-1.15×10^{-2}	8.11×10^{-4}	2×10^{-9}	1816	
row 3	-4.56×10^{-3}	-0.52	-0.72	-0.41	-2.49×10^{-2}	4.30×10^{-3}	3×10^{-9}	2117	
row 4	-2.59×10^{-2}	-7.08×10^{-2}	-0.40	-0.51	-0.22	$-7.54\ 10^{-3}$	6×10^{-7}	1740	
row 5	-8.43×10^{-4}	-1.16×10^{-2}	-2.48×10^{-2}	-0.22	0.82	0.16	2×10^{-5}	1626	
row 6	-3.96×10^{-5}	3.61×10^{-3}	6.33×10^{-3}	-9.09×10^{-3}	0.15	2.12	8×10^{-3}	953	

[a] We show the minimization without preconditioning only for the first row of the **R** matrix.

As seen in the Tables 3 and 4 and Figures 2 and 3, the number of conjugate gradient iteration steps decreases dramatically when the preconditioner is applied. Preconditioning finds a usually more accurate solution with substantially fewer iterations. The evolution of F with the number of iterations is shown in Figures 2 and 3.

5.C. The Wave Function. Previous work[47] has shown that the KVP might not give accurate results for the wave function throughout the interaction region. Since the KVP has been designed to compute scattering cross sections and these can often be more accurate than the wave function itself, this is not a fatal flaw. There are however a few problems where the wave function in the interaction region is needed. The MEM is designed specifically to make the wave function accurate at all grid points. Since we do not have exact wave functions for this model, we test the accuracy of the wave function by calculating the value of $\hat{H}\Psi - E\Psi$ at the grid points. The results of such calculations are shown in Figures 4 and 5 for the three- and the six-open-channel calculations, respectively.

In the case of the six-open-channel problem (Figure 5), the error occurs mainly at the open boundary, meaning that the crossover between the interaction and asymptotic wave function, eqs 7 and 11, is the source of the remaining error. However, the errors are very small (on the order of 10^{-6}). In the three-channel calculation (Figure 4), because a coarser grid was used, the error is larger, and the dominant error occurs at the border of the grid.

In Figures 6 and 7, we show the wave function itself for the three- and six-open-channel problems for the wave function that describes transitions from the ground state to the excited states (the top row of the **R** matrix). These figures show that the wave function is not visibly erroneous near the borders (it goes smoothly to zero except at the open boundary, where it is well-behaved). The error in Figure 4 comes instead from the tendency of the Chebyshev method for calculating derivatives (hence the kinetic energy in $\hat{H}\Psi$) to concentrate the error at the ends of the interval.[7,8] If necessary, this error can be decreased by increasing the basis set, as can be seen in Figure 5 for the six-channel case.

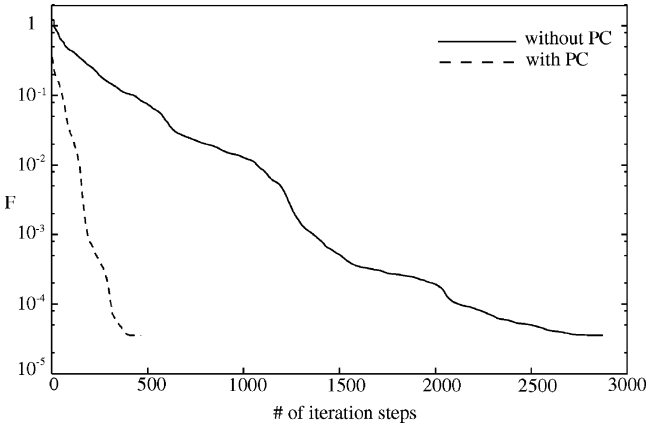

Figure 2. The convergence of the error for the system with three open channels and $N = M = 32$ as a function of the number of CG iterations, with and without preconditioning.

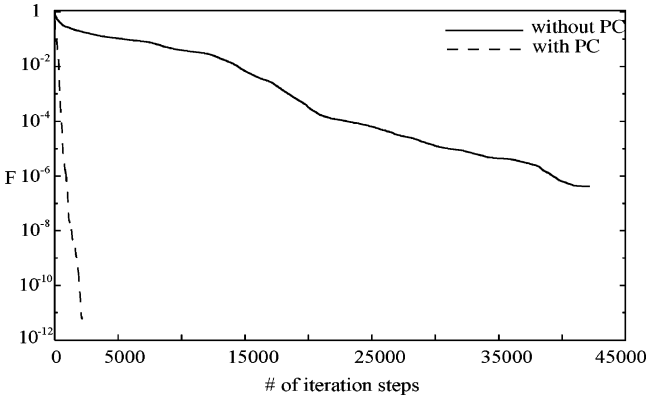

Figure 3. Same as that for Figure 2 but for the system with six open channels and $N = M = 64$.

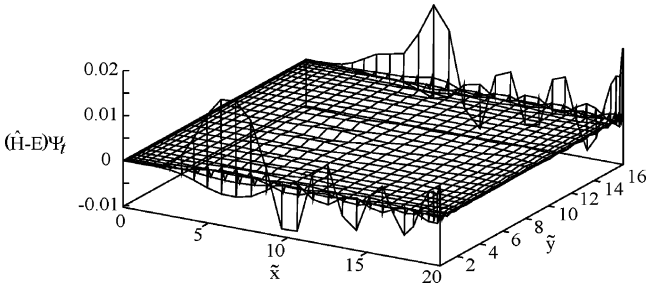

Figure 4. The magnitude of $(\hat{H} - E)\Psi_t$ at the grid points for the three-channel problem and $N = M = 32$.

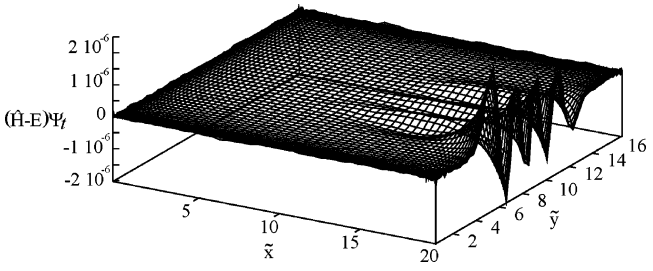

Figure 5. The magnitude of $(\hat{H} - E)\Psi_t$ at the grid points for the six-channel problem and $N = M = 64$.

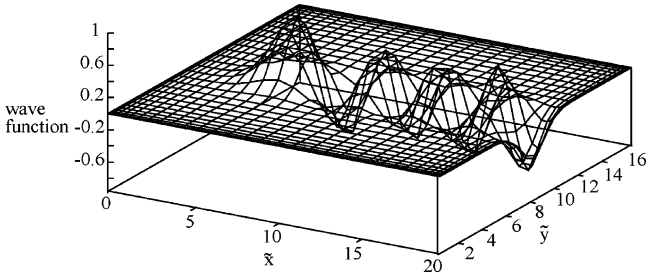

Figure 6. The wave function in the interaction region for $E = 3.0$ au and $N = M = 32$.

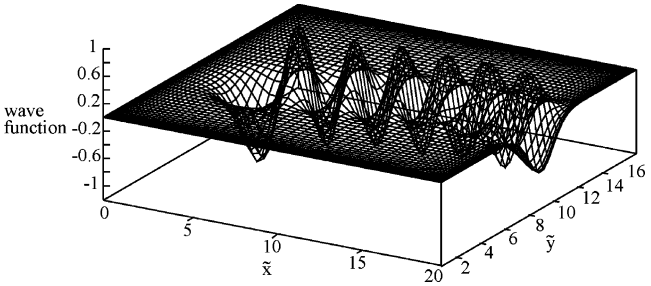

Figure 7. The wave function in the interaction region for $E = 6.0$ au and $N = M = 64$.

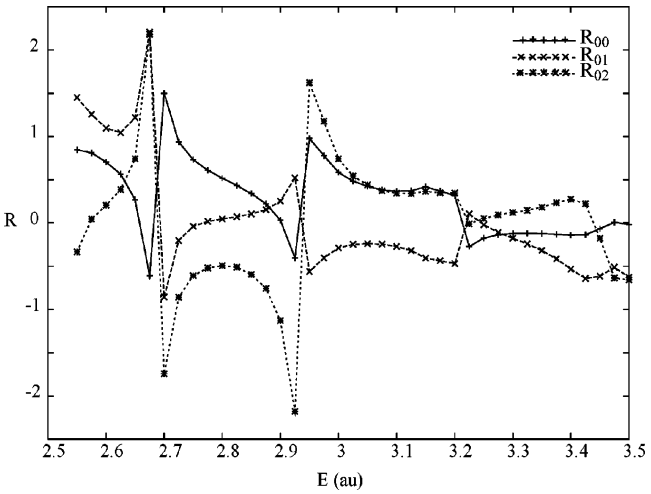

Figure 8. The dependence of the **R** matrix elements (R_{00}, R_{01}, R_{02}) on the incident energy for a system with several resonances (see text for details).

5.D. The Energy Dependence of the Cross Section. Several studies[62−64] have shown that the KVP with the **R** matrix form of the asymptotic wave functions is numerically unstable at certain energies and sometimes produces false resonances. For this reason, we check whether the MEM gives a reasonable energy dependence of the transition probabilities. For this purpose, we use an attractive Lennard-Jones potential for the $He-H_2$ interaction, with coordinates as those in eq 2

$$V_I(\tilde{x},\tilde{y}) = 20\left[-\left(\frac{6}{\tilde{x}-\tilde{y}}\right)^6 + \left(\frac{6}{\tilde{x}-\tilde{y}}\right)^{12}\right] \tag{33}$$

together with a harmonic oscillator potential for the internal motion of H_2

$$V_{12}(\tilde{y}) = \frac{1}{2}(\tilde{y}-\tilde{y}_{eq})^2 \tag{34}$$

Resonances occur at certain energies when the incoming atom forms a temporary bound state with the molecule. At these energies, the phase shifts (**R** matrix elements) tend to change rapidly with energy.[65] We show the resonances for a problem with three open channels in Figure 8. There are no instabilities at any of the energies used in this calculation, and the error converges to very small values.

6. Conclusions

We have proposed a new method for implementing the minimum error method using a pseudospectral representation of the wave function based on Chebyshev polynomials and a preconditioned conjugate gradient minimization of the error functional. Unlike the Kohn variational principle, the present method experiences no instability at any boundary conditions. The use of Chebyshev polynomials allows a fast and accurate calculation of the derivatives. The basis set is orthonormal and complete, and therefore, we are guaranteed to improve the accuracy as we increase the basis set. Also, because the present method involves searching for a minimum rather than a saddle point, a preconditioned conjugate gradient method is used instead of a matrix inversion, which allows the use of larger basis sets.

Acknowledgment. The authors gratefully acknowledge support by the Air Force Office for Scientific Research.

Appendix A

The Implementation of the Conjugate Gradient Minimization. The iterative minimization scheme starts with a guess $z^{(0)}$ for the values of the components of the vector z in eq 30, and generates a sequence $z^{(0)}$, $z^{(1)}$, ..., $z^{(k)}$,..., which converges to a value that minimizes $F(z)$. Each iteration starts with known (but approximate) values of z. This allows us to calculate $F(z)$ and the gradient of F at this particular value of z

$$\nabla F = \left\{\frac{\partial F}{\partial \Psi_{1,1}}, ..., \frac{\partial F}{\partial \Psi_{N-1,M-1}}, \frac{\partial F}{\partial R_{0,0}}, ..., \frac{\partial F}{\partial R_{0,m}}\right\} \tag{A1}$$

The calculation of $F(z)$ is explained in Appendix C and that of $\nabla F(z)$ in Appendix D.

One can show that F is bilinear in z

$$F = z^{\mathrm{T}}\mathbf{A}z + b^{\mathrm{T}}z + c \tag{A2}$$

where **A** is a positive definite matrix, and that this matrix is ill-conditioned; for $N = M = 32$, its largest eigenvalue exceeds the smallest by 7 orders of magnitude. Therefore, preconditioning the gradient is essential for the efficient convergence of the conjugate gradient search. Preconditioning requires that we find a similarity transformation that turns this matrix into one whose eigenvalues are of comparable magnitude with each other. There is no systematic prescription for doing this; preconditioning is an art form, with various recipes offered for different specific situations.[6] We use a method described in our previous work[47] and adapted to two dimensions. We write the preconditioned vector as

$$G^{(k)} = \hat{P}(-\nabla F^{(k)}) \tag{A3}$$

where $\hat{P}$ the preconditioning operator and $-\nabla F^{(k)}$ is the steepest descent direction at the point $z^{(k)}$.

Now, we use the present guess $z^{(k)}$ and the previous search direction $d^{(k-1)}$ to generate the new guess $z^{(k+1)}$. First, we calculate a new search direction $d^{(k)}$ using

$$d^{(k)} = G^{(k)} + \beta^{(k)}d^{(k-1)} \tag{A4}$$

and $\beta^{(k)}$ is calculated with

$$\beta^{(k)} = \frac{\nabla F^{(k)}\cdot G^{(k)}}{\nabla F^{(k-1)}\cdot G^{(k-1)}} \tag{A5}$$

Equation A5 is based on the standard formula[9] but altered in order to include preconditioning. Next, we set

$$z^{(k+1)} = z^{(k)} + \alpha^{(k)}d^{(k)} \tag{A6}$$

where $\alpha^{(k)}$ is the distance to the line minimum of $F(z)$ along the search direction $d^{(k)}$, that is, we choose $\alpha^{(k)}$ to minimize F_{new} in the formula

$$F_{new} = F(z^{(k)} + \alpha^{(k)} d^{(k)}) \tag{A7}$$

while holding the vectors $z^{(k)}$ and $d^{(k)}$ fixed. This line minimization is accomplished using Brent's method.[9]

The iteration scheme is initialized by guessing the values of $\Psi_t(1,1)$, ..., $\Psi_t(N-1,M-1)$, R_{01}, ..., R_{0m}. We do this by setting $\Psi_I(x,y) = 0$ in eq 7 and by giving (R_{00}, ..., R_{0m}) physically reasonable values. The efficiency of the scheme is not very sensitive to the initial guess.

Appendix B

How To Impose Efficiently the Condition $(d\Psi_I/dx)|_{x=x_{max}} = 0$. Imposing the boundary conditions is a delicate matter which is simplified considerably by using the values of the wave function as arguments in F. This allows us to fix the values of the wave function on the borders of the grid to satisfy the boundary conditions throughout the minimization iteration process. This means that we only need to optimize the values of the wave function inside of the grid, which reduces the number of variables in the minimization problem. Had we used the Chebyshev coefficients as the unknown quantities, we would have had to solve $2N + 2M$ linear equations for each CG iteration in order to obtain the correct boundary conditions.

Implementing the condition

$$\left.\frac{d\Psi_I(x,y_j)}{dx}\right|_{x=1} = 0 \tag{B1}$$

in eq 18 is more difficult and is done by a new procedure which is explained below.

Each new iteration (see Appendix A) produces numerical values for $\Psi_I(x_i,y_j)$ inside of the grid (the values at the border of the grid are kept fixed). To calculate the derivative with respect to x, at the point $x = 1$, we consider the Chebyshev expansion of $\Psi_I(x_i,y_j)$, take $(\partial/\partial x)$, and then set $x = 1$, with y fixed. The result is

$$\left[\frac{\partial\Psi_I(x,y_j)}{\partial x}\right]_{x=1} = \sum_{\alpha=0}^{N} c_\alpha(y_j)\left[\frac{dT_\alpha(x)}{dx}\right]_{x=1}\eta_\alpha = \sum_{\alpha=0}^{N} c_\alpha(y_j)\alpha^2\eta_\alpha \tag{B2}$$

where $\{c_\alpha(y_j)\}$ are the coefficients of the Chebyshev expansion of Ψ_I.

Next, we define the function $u(x)$, whose Chebyshev coefficients are α^2

$$u(x_i) = \sum_{\alpha=0}^{N} \eta_\alpha \alpha^2 T_\alpha(x_i) \tag{B3}$$

Then, one can show that

$$\left[\frac{\partial\Psi_I(x,y_j)}{\partial x}\right]_{x=1} = \sum_{i=0}^{N} \bar{u}(x_i)\Psi_I(x_i,y_j) \tag{B4}$$

with

$$\bar{u}(x_i) = \begin{cases} (2/N)u(x_i) & 0 < i < N \\ 0 & i = 0 \text{ or } N \end{cases} \tag{B5}$$

Note that $\bar{u}(x_i)$ needs to be calculated only once. The boundary condition eq B1 is imposed by replacing $\Psi_I(x_i,y_j)$ with a new function $\bar{\Psi}_I(x_i,y_j)$ which obeys eq B1. The new function is constructed by

$$\bar{\Psi}_I(x_i,y_j) = \Psi_I(x_i,y_j) - \bar{u}(x_i)\frac{\sum_{p=0}^{N}\bar{u}(x_p)\Psi_I(x_p,y_j)}{\sum_{p=0}^{N}\bar{u}(x_p)\bar{u}(x_p)} \tag{B6}$$

Now $\bar{\Psi}_I(x_i,y_j)$ has a zero derivative at the open boundary (at all values of y) since it makes the sum in eq B4 equal to zero. In addition, it remains zero on the borders of the interval since $\bar{u}(x_i)$ and $\Psi_I(x_i,y_j)$ are zero on the border. $\bar{\Psi}_I(x_i,y_j)$ satisfies therefore all boundary conditions and will be used as input in the next CG iteration. The same method is used on the steepest descent direction and the preconditioned vector, $-\nabla F^{(k)}$ and $G^{(k)}$, before they are used in eqs A3−A5.

Appendix C

The Evaluation of the Error Functional *F*. The only subtlety in evaluating the F is the efficient calculation of the derivatives in the kinetic energy operator when we know the values of the wave function on the grid. We illustrate briefly here the procedure by showing how we evaluate the derivative $\partial\Psi(x,y_j)/\partial x$ at the point $x = x_i$. We represent first the function as a Chebyshev sum

$$\Psi_t(x,y_j) = \sum_{\alpha=0}^{N} \eta_\alpha c_\alpha(y_j) T_\alpha(x) \tag{C1}$$

The coefficients $\{c_\alpha(y_j)\}$ are calculated from eq 24 with a FCT, in $O(N \log N)$ operations. Then, the coefficients $\{d_\alpha(y_j)\}$ of the derivative

$$\left[\frac{\partial\Psi_t(x,y_j)}{\partial x}\right]_{x=x_i} = \sum_{\alpha=0}^{N} \eta_\alpha\, d_\alpha(y_j) T_\alpha(x) \tag{C2}$$

are obtained from the recursion relation

$$d_N(y_j) = 0 \qquad d_{N-1}(y_j) = Nc_N(y_j)$$
$$d_\alpha(y_j) = d_{\alpha+2}(y_j) + 2kc_{\alpha+1}(y_j) \qquad \alpha = N-2, ..., 0 \tag{C3}$$

which requires $O(N)$ operations, and an inverse FCT gives the values of the derivative at each grid point $\{x_i\}$. For the second derivative in the kinetic energy operator, we apply eq C3 twice and then the inverse FCT.

Appendix D

The Evaluation of the Gradient of *F*. To minimize the functional F given by eq 28, we must take the derivative of F with respect to $\Psi_I(x_n,y_m)$ and the elements of the **R** matrix for some guess of these values, written as the vector z in eq 30. F is a bilinear function of these variables, and this should make taking the derivative a simple matter. Unfortunately, the kinetic energy contains terms such as $[\partial^2\Psi_t(x,y_j)/\partial x^2]_{x=x_i}$, and taking the derivative of this number with respect to $\Psi_I(x_n,y_m)$ must be done with care, especially because efficiency and accuracy are

important. We present here a method that avoids matrix multiplication (it involves $O(N \log N)$ operations not $O(N^2)$) and is very accurate.

Taking the derivative of F in eq 28 leads to

$$\frac{\partial F}{\partial \Psi_I(x_n,y_m)} = 2\sum_{i=0}^{N}\sum_{j=0}^{M} f(x_i,y_j)\left[\frac{\partial}{\partial \Psi_I(x_n,y_m)}((\hat{H}-E)\Psi_t)_{i,j}\right] \tag{D1}$$

with

$$f(x_i,y_j) = w_i w_j[(\hat{H}-E)\Psi_t]_{i,j} \tag{D2}$$

The difficult part in evaluating eq D1 is the derivative of the terms containing the kinetic energy. We will explain how this calculation is done for the term

$$A(n,m) = \sum_{i=0}^{N}\sum_{j=0}^{M} f(x_i,y_j)\left[\frac{\partial(\mathrm{d}^2\Psi_t/\mathrm{d}x^2)_{i,j}}{\partial \Psi_I(x_n,y_m)}\right] \tag{D3}$$

which is present when eq D1 is expanded. Let us assume for the moment that we can write

$$\left[\frac{\mathrm{d}\Psi_t(x,y_j)}{\mathrm{d}x}\right]_{x=x_i} = \sum_{p=0}^{N} D_{ip}\Psi_t(x_p,y_j) \tag{D4}$$

where D_{ip} are the elements of a matrix which is independent of y_j (to be determined shortly). Successive applications of eq D4 give

$$\left[\frac{\mathrm{d}^2\Psi_t(x,y_j)}{\mathrm{d}x^2}\right]_{x=x_i} = \sum_{q=0}^{N}\sum_{p=0}^{N} D_{iq}D_{qp}\Psi_t(x_p,y_j) \tag{D5}$$

Using eq D5, we can write eq D3 as

$$A(n,m) = \sum_{i=0}^{N}\sum_{j=0}^{M} f(x_i,y_j)\left(\left[\frac{\partial}{\partial \Psi_I(x_n,y_m)}\right]\right)\sum_{q=0}^{N}\sum_{p=0}^{N} D_{iq}D_{qp}\Psi_t(x_p,y_j) \tag{D6}$$

Taking the derivative through the last two summation signs and referring to the wave function expansion described by eqs 7 and 11 gives a Kronecker delta (a contribution of zero unless $n = p$ and $m = j$) and leads to

$$A(n,m) = \sum_{i=0}^{N} (DD)^{\mathrm{T}}_{ni} f(x_i,y_m) \tag{D7}$$

where $(DD)^{\mathrm{T}}_{ni}$ is the (n,i) element of the transpose of the matrix product **DD**.

We show next that the matrix **D**, defined by eq D4, exists, and then, we will present an iterative procedure that evaluates the sum in eq D5 much more efficiently than matrix multiplication.

To prove eq D4 and thus define the matrix **D**, we use eqs C1 and C2. The recurrence relation in eq 24 is equivalent to

$$d_\beta(y_j) = \sum_{\alpha=\beta+1}^{N} 2\alpha c_\alpha(y_j) \qquad \alpha - \beta \text{ odd} \tag{D8}$$

and eq D8 defines implicitly a matrix **M** such that

$$d_\beta(y_j) = \sum_{\gamma=0}^{N} M_{\beta\gamma}c_\gamma(y_j) \tag{D9}$$

The matrix **M** does not depend on y. Introducing this into eq D7 and using also, in eq D9, the inversion formula eq 24 gives

$$D_{ip} = \frac{2}{N}\sum_{\beta=0}^{N}\sum_{\gamma=0}^{N} T_\beta(x_i)M_{\beta\gamma}T_\gamma(x_p)\eta_p\eta_i \tag{D10}$$

Therefore, the matrix **D** exists, and it is defined by eq D10. This could be used to evaluate **D** and then in eq D7 to calculate $A(n,m)$. However, this would not be an efficient procedure since matrix multiplication is slow. It is possible to calculate **A** through several steps each performed in $O(N)$ operations. For this, we use the following recipe. To evaluate an expression of the form

$$\phi(x_n,y_m) = \sum_{i=0}^{N} D^{\mathrm{T}}_{ni} f(x_i,y_m) \tag{D11}$$

represent $f(x_i,y_m)$ by the Chebyshev sum

$$f(x_i,y_m) = \sum_{\alpha=0}^{N} g_\alpha(y_m)\, T_\alpha(x_i)\eta_\alpha \tag{D12}$$

Then, $\phi(x_n,y_m)$ is given by

$$\phi(x_n,y_m) = \sum_{\beta=0}^{N} h_\beta(y_m)\, T_\beta(x_i)\eta_\beta \tag{D13}$$

with coefficients $\{h_\beta(y_m)\}$ obtained from $\{g_\alpha(y_m)\}$ by the following recursion relations

$$e_0 = 0$$

$$e_1 = g_0$$

$$e_{\alpha+1} = e_{\alpha-1} + 2g_\alpha \qquad \alpha = 2, ..., N-1$$

$$h_\alpha = \alpha e_\alpha \qquad \alpha = 0, ..., N \tag{D14}$$

Applying this recursion twice gives $A(n,m)$ in eq D7 in $O(N)$ operations. A formal proof of this recurrence relation is very tedious and will not be given here. One can verify numerically that the scheme works.

The functional derivatives of the other terms involving kinetic energy are calculated similarly. The terms that do not involve the kinetic energy and those involving derivatives of F with respect to the **R** matrix elements are straightforward to calculate.

References and Notes

(1) Althorpe, S. C.; Clary, D. C. *Annu. Rev. Phys. Chem.* **2003**, *54*, 493.
(2) Hu, W.; Schatz, G. C. *J. Chem. Phys.* **2006**, *125*.
(3) Secrest, D.; Johnson, B. R. *J. Chem. Phys.* **1966**, *45*, 4556.
(4) Secrest, D.; Eastes, W. *J. Chem. Phys.* **1972**, *56*, 2502.
(5) Rivlin, T. J. *An Introduction to the Approximation of Functions*, 2nd ed.; Dover: Mineola, NY, 1981.
(6) Canuto, C.; Hussaini, M.; Quarteroni, A.; Zang, T. *Spectral Methods in Fluid Dynamics*, 3rd ed.; Springer: Berlin, Germany, 1991.
(7) Boyd, J. P. *Chebyshev and Fourier Spectral Methods*, 2nd ed.; Dover: Mineola, NY, 2001.
(8) Mason, J. C.; Handscomb, D. C. *Chebyshev Polynomials*; CRC Press: Boca Raton, FL, 2003.
(9) Press, W. H.; Teukolsky, S. A.; Vetterling, W. T.; Flannery, B. P. *Numerical Recipes*, 2nd ed.; Cambridge University Press: New York, 2001.
(10) Miller, W. H. *J. Phys. Chem. A* **1998**, *102*, 793.

(11) Yang, Z.; Tackett, A.; Di Ventra, M. *Phys. Rev. B* **2002**, *66*, 041405.
(12) Kohn, W. *Phys. Rev.* **1948**, *74*, 1763.
(13) Schwenke, D. W.; Haug, K.; Truhlar, D. G.; Sun, Y.; Zhang, J. Z. H.; Kouri, D. J. *J. Phys. Chem.* **1987**, *91*, 6080.
(14) Miller, W. H.; Jansen op de Haar, B. M. D. D. *J. Chem. Phys.* **1987**, *86*, 6213.
(15) Peet, A. C.; Miller, W. H. *Chem. Phys. Lett.* **1988**, *149*, 257.
(16) Duneczky, C.; Wyatt, R. E. *J. Chem. Phys.* **1988**, *89*, 1448.
(17) Zhang, J. Z. H.; Miller, W. H. *Chem. Phys. Lett.* **1987**, *140*, 329.
(18) Zhang, J. Z. H.; Chu, S. I.; Miller, W. H. *J. Chem. Phys.* **1988**, *88*, 6233.
(19) Zhang, J. Z. H.; Miller, W. H. *Chem. Phys. Lett.* **1988**, *153*, 465.
(20) Zhang, J. Z. H.; Miller, W. H. *J. Chem. Phys.* **1988**, *88*, 4549.
(21) Zhang, J. Z. H.; Kouri, D. J.; Haug, K.; Schwenke, D. W.; Shima, Y.; Truhlar, D. G. *J. Chem. Phys.* **1988**, *88*, 2492.
(22) Zhang, J. Z. H.; Miller, W. H. *J. Chem. Phys.* **1989**, *91*, 1528.
(23) Yang, W.; Peet, A. C.; Miller, W. H. *J. Chem. Phys.* **1989**, *91*, 7537.
(24) Mielke, S. L.; Truhlar, D. G.; Schwenke, D. W. *J. Chem. Phys.* **1991**, *95*, 5930.
(25) Saalfrank, P.; Miller, W. H. *J. Chem. Phys.* **1993**, *98*, 9040.
(26) Tawa, G. J.; Mielke, S. L.; Truhlar, D. G.; Schwenke, D. W. *J. Chem. Phys.* **1994**, *100*, 5751.
(27) Mielke, S. L.; Truhlar, D. G.; Schwenke, D. W. *J. Chem. Phys.* **1994**, *98*, 1053.
(28) Heidinger, L. E. *Surf. Sci.* **2000**, *444*, 87.
(29) Rudge, M. R. H. *J. Phys. B* **1976**, *9*, 2357.
(30) Rudge, M. R. H. *J. Phys. B* **1990**, *23*, 4275.
(31) Rudge, M. R. H. *J. Phys. A* **2003**, *36*, 1485.
(32) Bardsley, J. N.; Gerjuoy, E.; Sukumar, C. V. *Phys. Rev. A* **1972**, *6*, 1813.
(33) Read, F. H.; Soto-Montiel, J. R. *J. Phys. B* **1973**, *6*, L15.
(34) Abdelraouf, M. A. *J. Phys. B* **1979**, *12*, 3349.
(35) Abdelraouf, M. A. *Phys. Rep.* **1982**, *84*, 163.
(36) Merts, A. L.; Collins, L. A. *J. Phys. B* **1985**, *18*, L29.
(37) Apagyi, B.; Ladanyi, K. *Phys. Rev. A* **1986**, *33*, 182.
(38) McCurdy, C. W.; Rescigno, T. N. *Phys. Rev. A* **1989**, *40*, 1297.
(39) Chatfield, D. C.; Reeves, M. S.; Truhlar, D. G.; Duneczky, C.; Schwenke, D. W. *J. Chem. Phys.* **1992**, *97*, 8322.
(40) Reeves, M. S.; Chatfield, D. C.; Truhlar, D. G. *J. Chem. Phys.* **1993**, *99*, 2739.
(41) Groenenboom, G. C.; Colbert, D. T. *J. Chem. Phys.* **1993**, *99*, 9681.
(42) Peskin, U.; Edlund, A.; Bar-On, I.; Galperin, M.; Nitzan, A. *J. Chem. Phys.* **1999**, *111*, 7558.
(43) Mott, N. F.; Massey, H. S. *The Theory of Atomic Collisons*, 3rd ed.; Clarendon Press: Oxford: U.K., 1965.
(44) Gottlieb, D.; Orszag, S. A. *Numerical Analysis of Spectral Methods: Theory and Applications*; SIAM: Philadelphia, PA, 1977.
(45) Mund, E. H. *Appl. Numer. Math.* **2000**, *33*, 61.
(46) Poirier, B.; Miller, W. H. *Chem. Phys. Lett.* **1997**, *265*, 77.
(47) Temel, B.; Mills, G.; Metiu, H. *J. Phys. Chem. A* **2006**, *110*, 10513.
(48) Huang, Y.; Iyengar, S. S.; Kouri, D. J.; Hoffman, D. K. *J. Chem. Phys.* **1996**, *105*, 927.
(49) Jang, H. W. *Theor. Chem. Acc.* **1998**, *99*, 420.
(50) Neuhauser, D. *J. Chem. Phys.* **1996**, *103*, 8513.
(51) Muga, J. G.; Palao, J. P.; Navarro, B.; Egusquiza, I. L. *Phys. Rep.* **2004**, *395*, 357.
(52) Halasz, G. J.; Vibok, A. *Chem. Phys. Lett.* **2000**, *323*, 287.
(53) Shemer, O.; Brisker, D.; Moiseyev, N. *Phys. Rev. A* **2005**, *71*, 032716.
(54) Moiseyev, N. *Phys. Rep.* **1998**, *302*, 211.
(55) Light, J. C.; Hamilton, I. P.; Lill, J. V. *J. Chem. Phys.* **1985**, *82*, 1400.
(56) Colbert, D. T.; Miller, W. H. *J. Chem. Phys.* **1992**, *96*, 1982.
(57) Fornberg, B.; Sloan, D. M. A review of Pseudospectral Methods for Solving Partial Differential Equations. In *Acta Numerica 1994*; Iserles, A., Ed.; Cambridge: New York, 1994.
(58) Gottlieb, D.; Shu, C. W. *SIAM Rev.* **1997**, *39*, 644.
(59) Jaquet, R.; Kumpf, A.; Heinen, M. *J. Chem. Soc., Faraday Trans.* **1997**, *93*, 1027.
(60) Grozdanov, T. P.; McCarroll, R. *J. Chem. Phys.* **2007**, *126*, 034310.
(61) Gutschick, V. P.; McKoy, V.; Diestler, D. J. *J. Chem. Phys.* **1970**, *52*, 4807.
(62) Schwartz, C. *Ann. Phys.* **1961**, *16*, 36.
(63) Nesbet, R. K. *Phys. Rev.* **1968**, *175*, 134.
(64) Nesbet, R. K. *Variational Methods in Electron-Atom Scattering Theory*; Plenum: New York, 1980.
(65) Joachain, C. J. *Quantum Collision Theory*, 3rd ed.; Elsevier Science Publishers: Amsterdam, The Netherlands, 1983.